



# Impact of Consciousness Energy Healing Treatment on the Physicochemical and Thermal Properties of Chromium Trioxide ( $\text{CrO}_3$ )

Dahryn Trivedi<sup>1</sup>, Mahendra KT<sup>1</sup>, Alice Branton<sup>1</sup>, Gopal Nayak<sup>1</sup> and Snehasis Jana<sup>2\*</sup>

<sup>1</sup>Trivedi Global, Inc., Henderson, USA

<sup>2</sup>Trivedi Science Research Laboratory Pvt. Ltd., India

**\*Corresponding author:** Snehasis Jana, Trivedi Science Research Laboratory Pvt. Ltd., Thane (W), India. Tel: +91-022-25811234; Email: publication@trivedieffect.com

**Received Date:** March 18, 2019; **Published Date:** March 28, 2019

## Abstract

Chromium trioxide ( $\text{CrO}_3$ ) is a very hygroscopic, toxic and powerful oxidizing material. It has many industrial applications. The purpose of this study was to evaluate the influence of the Consciousness Energy Healing Treatment (the Trivedi Effect<sup>®</sup>) on the physicochemical properties of  $\text{CrO}_3$  using PSA, PXRD, and DSC analytical techniques. The  $\text{CrO}_3$  test sample was divided into two parts. One part of  $\text{CrO}_3$  was considered as a control sample (no Biofield Energy Treatment was provided), while other parts of  $\text{CrO}_3$  received the Consciousness Energy Healing Treatment remotely by a distinguished Biofield Energy Healer, Dahryn Trivedi and termed as a treated sample. The particle size values of the treated  $\text{CrO}_3$  were increased by 71.13% ( $d_{10}$ ), 2.09% ( $d_{50}$ ), and 0.03% {D (4, 3)}, but decreased by 10.86% at  $d_{90}$  compared to the control sample. The specific surface area of the treated  $\text{CrO}_3$  was significantly decreased by 63.76% compared with the control sample. The powder XRD peak intensities and crystallite sizes of the treated  $\text{CrO}_3$  were significantly altered ranging from -27.64% to 30.72% and -46.14% to 136.44%, respectively; however, the average crystallite size was significantly increased by 17.65% compared with the control sample. The latent heat of fusion the treated  $\text{CrO}_3$  powder was significantly increased by 16.02% compared with the control sample. The experimental results indicated that the Trivedi Effect<sup>®</sup>-Consciousness Energy Healing Treatment might have included a new polymorphic form of  $\text{CrO}_3$  which may show better powder flowability and lower solubility. Thus, it may lower the absorption and toxicity of  $\text{CrO}_3$  on inhalation, ingestion, contact to skin and eye, chronic exposure, and aggravation of pre-existing conditions. As well the Dahryn's Consciousness Energy Healing Treated  $\text{CrO}_3$  would be very useful for the industry manufacturing the synthetic rubies, aerospace parts, stripping agent of anodic coatings, etc.

**Keywords:** Chromium trioxide; The Trivedi Effect<sup>®</sup>; Consciousness Energy Healing Treatment; Particle size; Surface area; PXRD; DSC

**Abbreviations:** NIH: National Institutes of Health; NCCAM: National Center for Complementary and Alternative Medicine; PSA: Particle Size Analysis; PXRD:

Powder X-Ray Diffraction; DSC: Differential Scanning Calorimetry; SSA: Specific Surface Area; FWHM: Full-Width At Half Maximum.

## Introduction

Chromium trioxide {chromium (VI) oxide or CrO<sub>3</sub>} is chemically an acidic anhydride of chromic acid. The CrO<sub>3</sub> is highly hygroscopic, toxic, and a powerful oxidizer. It will ignite the organic materials on contact. It is typically employed for the chrome plating and it generates passivating chromate films by reacting with zinc, cadmium, and other metals to resist the process of corrosion [1-3]. It is also used for the manufacture of synthetic rubies, aerospace parts, and stripping agent of anodic coatings [2,4]. The CrO<sub>3</sub> is highly corrosive, toxic, and carcinogenic. It causes potential health effects on inhalation, ingestion, contact with the skin and eye, chronic exposure, and aggravation of pre-existing conditions [5].

Physicochemical properties of any substance are very important for the application purpose. The Trivedi Effect®-Biofield Energy Healing Treatment scientifically proved that it has a huge impact to alter the intrinsic physicochemical properties of various living and non-living objects [6-9]. The Trivedi Effect® is a natural and only scientifically proven phenomenon in which a person can harness this inherently intelligent energy from the Universe and transmit it anywhere on the planet. It was believed that the Trivedi Effect® act through the possible mediation of neutrinos oscillation [10]. Every living organism possesses a unique para-dimensional electromagnetic field around the body which originates from the continuous movements of the charged particles, ions, cells, blood/lymph flow, brain functions, and heart function in the body known as "Biofield Energy". Biofield based Energy Healing Therapies (energy medicine) have been reported with significant outcomes against various disease conditions [11]. The National Institutes of Health (NIH) and National Center for Complementary and Alternative Medicine (NCCAM) recommend and included the Energy therapy under Complementary and Alternative Medicine (CAM) category along with Tai Chi, Qi Gong, Ayurvedic medicine, traditional Chinese medicines, homeopathy, chiropractic/osteopathic manipulation, Reiki, healing touch, yoga, meditation, special diets, massage, guided imagery, acupuncture, acupressure, hypnotherapy, Rolfing structural integration, mindfulness, cranial sacral therapy, and applied prayer. The CAM therapy has been accepted by the most of the U.S. people [12,13]. With this respects, the Trivedi Effect®-Consciousness Energy Healing Treatment also been comprehensively reported with amazing results in the field of material science [14,15], organic chemistry [16,17], nutraceutical/pharmaceutical sciences [6-8,18,19], agriculture [9,20], biotechnology [21,22], microbiology [23,24], and medical science [25].

Considering the outstanding results, the current study has been designed to evaluate the impact of the Trivedi Effect®-Consciousness Energy Healing Treatment on CrO<sub>3</sub> using particle size analysis (PSA), powder X-ray diffraction (PXRD), and differential scanning calorimetry (DSC) analytical techniques.

## Materials and Methods

### Chemicals and reagents

The test sample CrO<sub>3</sub> powder was obtained from Sigma Aldrich, India and all other chemicals used during the experiments were of the analytical grade also procured in India.

### Consciousness energy healing treatment strategies

The CrO<sub>3</sub> powder considered for the experiment was divided into two parts. The Trivedi Effect®-Consciousness Energy Healing Treatment was received by one part of the test sample remotely under standard laboratory conditions for 3 minutes by the renowned Biofield Energy Healer, Dahryn Trivedi, USA, and known as the treated sample. However, another part of the test item was treated with a "sham" healer and considered as a control (untreated) sample. The "sham" healer is totally ignorant about the Biofield Energy Treatment. After the treatment, the treated and untreated samples were kept in sealed conditions and characterized using PSA, PXRD, and DSC analytical techniques.

### Characterization

**Particle size analysis (PSA):** The particle size analysis of CrO<sub>3</sub> powder was performed on Malvern Mastersizer 2000, from the UK [26, 27]. The % change in particle size (d) for CrO<sub>3</sub> powder was calculated using the following equation 1:

$$\% \text{ change in particle size} = \frac{[d_{\text{Treated}} - d_{\text{Control}}]}{d_{\text{Control}}} \times 100 \quad (1)$$

Where  $d_{\text{Control}}$  and  $d_{\text{Treated}}$  are the particle size ( $\mu\text{m}$ ) for at below 10% level ( $d_{10}$ ), 50% level ( $d_{50}$ ), and 90% level ( $d_{90}$ ) of the control and the Biofield Energy Treated samples, respectively.

The % change in surface area (S) was calculated using the following equation 2:

$$\% \text{ change in surface area} = \frac{[S_{\text{Treated}} - S_{\text{Control}}]}{S_{\text{Control}}} \times 100 \quad (2)$$

Where  $S_{\text{Control}}$  and  $S_{\text{Treated}}$  are the surface area of the control and the Biofield Energy Treated CrO<sub>3</sub>, respectively.

**Powder X-ray diffraction (PXRD) analysis:** The PXRD analysis of CrO<sub>3</sub> was performed with the help of Rigaku

MiniFlex-II Desktop X-ray diffractometer (Japan) [28, 29]. The average size of individual crystallites was calculated using the Scherrer's formula (3)

$$G = k\lambda/\beta\cos\theta \quad (3)$$

Where  $k$  is the equipment constant (0.94),  $G$  is the crystallite size in nm,  $\lambda$  is the radiation wavelength (0.154056 nm for  $K\alpha_1$  emission),  $\beta$  is the full-width at half maximum (FWHM), and  $\theta$  is the Bragg angle [30].

The % change in crystallite size ( $G$ ) of  $\text{CrO}_3$  was calculated using the following equation 4:

$$\% \text{ change in crystallite size} = \frac{[G_{\text{Treated}} - G_{\text{Control}}]}{G_{\text{Control}}} \times 100 \quad (4)$$

Where  $G_{\text{Control}}$  and  $G_{\text{Treated}}$  are the crystallite size of the control and the Biofield Energy Treated samples, respectively.

**Differential scanning calorimetry (DSC):** The DSC analysis of  $\text{CrO}_3$  was performed with the help of DSC Q200, TA instruments [26, 27]. The % change in melting point ( $T$ ) was calculated using the following equation 5:

$$\% \text{ change in melting point} = \frac{[T_{\text{Treated}} - T_{\text{Control}}]}{T_{\text{Control}}} \times 100 \quad (5)$$

Where  $T_{\text{Control}}$  and  $T_{\text{Treated}}$  are the melting point of the control and treated samples, respectively.

The % change in the latent heat of fusion ( $\Delta H$ ) was calculated using the following equation 6:

$$\% \text{ change in latent heat of fusion} = \frac{[\Delta H_{\text{Treated}} - \Delta H_{\text{Control}}]}{\Delta H_{\text{Control}}} \times 100$$

(6)

Where  $\Delta H_{\text{Control}}$  and  $\Delta H_{\text{Treated}}$  are the latent heat of fusion of the control and the Biofield Energy Treated  $\text{CrO}_3$ , respectively.

## Results and Discussion

### Particle size analysis (PSA)

The PSA analysis data of both the control and the Biofield Energy Treated  $\text{CrO}_3$  powder are presented in Table 1. The particle size values in the Biofield Energy Treated  $\text{CrO}_3$  powder was increased at  $d_{10}$ ,  $d_{50}$ , and  $D(4,3)$  by 71.13%, 2.09%, and 0.03%, respectively compared to the control sample. However, at  $d_{90}$  the particle size was decreased by 10.86% in the Biofield Energy Treated sample compared to the control sample. The specific surface area (SSA) of the treated  $\text{CrO}_3$  powder (0.0216  $\text{m}^2/\text{g}$ ) was significantly decreased by 63.76% compared with the control sample (0.0596  $\text{m}^2/\text{g}$ ). From the results, it can be assumed that the Consciousness Energy Healing Treatment might be responsible for reducing internal force for increasing the particle size of  $\text{CrO}_3$  sample, hence decreased the surface area significantly. Increased in the particle size of the compound may help in enhancing the appearance, shape, and flow ability of the compound [31, 32]. Hence, the Biofield Energy Treated  $\text{CrO}_3$  might improve the powder flow ability, lower solubility, lower the absorption, and lower toxicity due to inhalation, ingestion, contact to skin and eye, chronic exposure, and aggravation of pre-existing conditions.

Parameter	$d_{10}$ ( $\mu\text{m}$ )	$d_{50}$ ( $\mu\text{m}$ )	$d_{90}$ ( $\mu\text{m}$ )	$D(4,3)$ ( $\mu\text{m}$ )	SSA ( $\text{m}^2/\text{g}$ )
Control	107.60	326.69	634.25	354.85	0.0596
Biofield Energy Treated	184.13	333.51	565.36	354.98	0.0216
Percent change* (%)	71.13	2.09	-10.86	0.03	-63.76

Table 1: Particle size distribution of the control and the Biofield Energy Treated  $\text{CrO}_3$  powder.

$d_{10}$ ,  $d_{50}$ , and  $d_{90}$ : particle diameter corresponding to 10%, 50%, and 90% of the cumulative distribution,  $D(4,3)$ : the average mass-volume diameter, and SSA: the specific surface area. \*denotes the percentage change in the Particle size distribution of the Biofield Energy Treated sample with respect to the control sample.

### Powder X-ray diffraction (PXRD) analysis

The sharp and intense peaks in the PXRD diffractograms of both the control and the Biofield Energy Treated  $\text{CrO}_3$  powder samples (Figure 1) indicated that both the samples were crystalline. The highest peak intensity of both the samples was found at  $2\theta$  equal to  $21.2^\circ$  (Table 2, entry 1). Overall, the peak intensities of the Biofield Energy Treated  $\text{CrO}_3$  sample were significantly altered

ranging from -27.64% to 30.72% compared to the control sample.

Likewise, the average crystallite sizes of the treated  $\text{CrO}_3$  were significantly altered ranging from -46.14% to 136.44% compared to the control sample. Overall, the average crystallite size of the Biofield Energy Treated  $\text{CrO}_3$  (675 nm) was significantly increased by 17.65% compared with the control sample (573.75 nm).

Entry No.	Bragg angle ( $2\theta$ )		Peak Intensity (%)			Crystallite size (G, nm)		
	Control	Treated	Control	Treated	% change <sup>a</sup>	Control	Treated	% change <sup>b</sup>
1	21.22	21.19	123	89	-27.64	596	321	-46.14
2	25.95	25.88	54.7	57	4.20	467	504	7.92
3	26.35	26.29	30.6	40	30.72	609	402	-33.99
4	37.45	37.41	24.5	23.4	-4.49	623	1473	136.44
5	Average crystallite size					573.75	675	17.65

Table 2: PXRD data for the control and the Biofield Energy Treated  $\text{CrO}_3$  powder.

<sup>a</sup>denotes the percentage change in the peak intensity of the Biofield Energy Treated sample with respect to the control sample; <sup>b</sup>denotes the percentage change in the crystallite size of the Biofield Energy Treated sample with respect to the control sample.

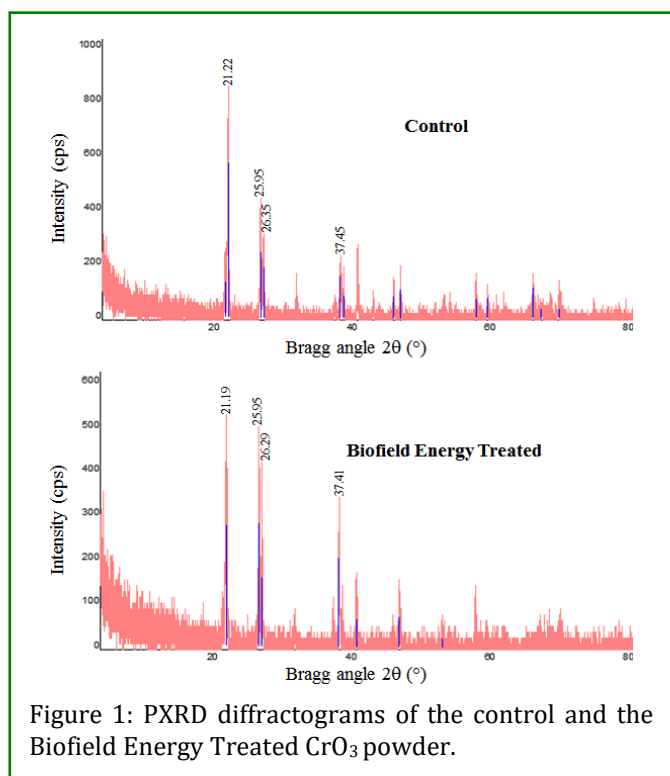


Figure 1: PXRD diffractograms of the control and the Biofield Energy Treated  $\text{CrO}_3$  powder.

From the results, it was found that the crystallite sizes and peak intensities of the Biofield Energy Treated sample were significantly altered compared to the control sample. The peak intensity of any diffraction face on the crystalline compound changes according to the crystal morphology [33] and alterations in the PXRD pattern provide the proof of polymorphic transitions [34, 35]. The Trivedi Effect<sup>®</sup> probably produced the new polymorphic form of  $\text{CrO}_3$  *via* neutrino oscillations [10]. Different polymorphic forms of a compound have significant effects on their physicochemical and thermal properties like melting point, energy, stability, and solubility [36, 37]. Therefore, it can be assumed that the Biofield Energy Treated  $\text{CrO}_3$  would be more useful for the industry as a raw material for manufacturing.

### Differential scanning calorimetry (DSC) analysis

The thermal analysis of  $\text{CrO}_3$  powder has been performed to characterize and compare the thermal behavior of the Biofield Energy Treated sample compared to the control sample (Figure 2). The control and the Biofield Energy Treated  $\text{CrO}_3$  powder showed the sharp endothermic peak at 199.24°C and 201.48°C, respectively (Table 3). The melting point of the Biofield Energy Treated  $\text{CrO}_3$  powder was slightly increased by 1.12% compared with the control sample (Table 3).

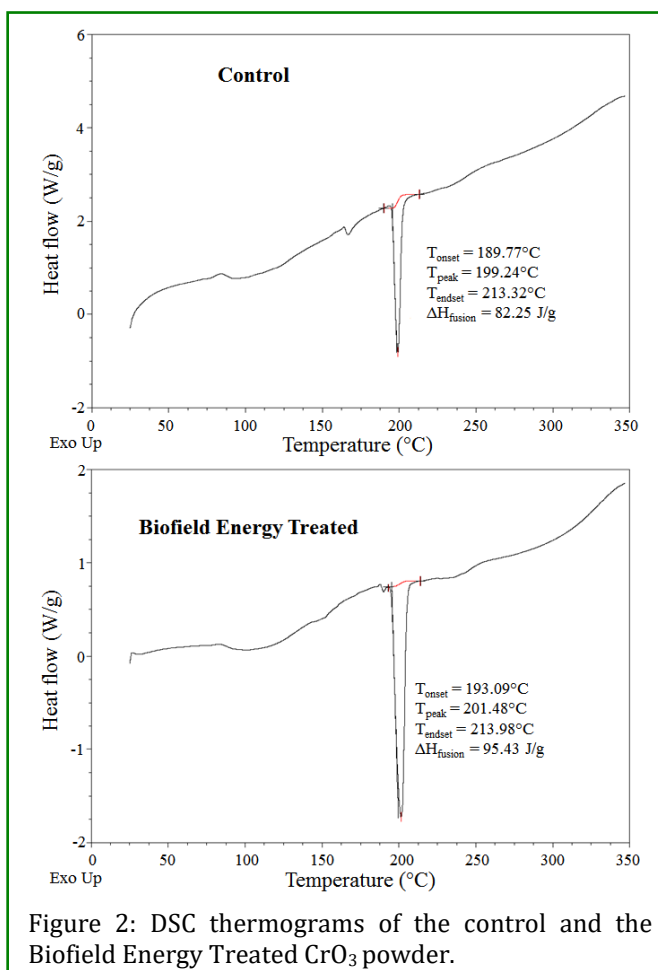


Figure 2: DSC thermograms of the control and the Biofield Energy Treated  $\text{CrO}_3$  powder.

The heat energy required to melt (latent heat of fusion;  $\Delta H_{\text{fusion}}$ ) the Biofield Energy Treated  $\text{CrO}_3$  powder (95.43 J/g) was significantly increased by 16.02% compared with the control sample (82.25 J/g) (Table 3). The change in the latent heat of fusion can be due to the disrupted molecular chains and the crystal structure [38]. Therefore, it can be presumed that Dahryn's Biofield Energy Treatment (the Trivedi Effect®) might be responsible for the stronger intermolecular chains and crystal structure of  $\text{CrO}_3$  which would improve the thermal stability of the treated sample compared with the control sample.

Sample	Melting point (°C)	$\Delta H$ (J/g)
Control Sample	199.24	82.25
Biofield Energy Treated	201.48	95.43
% Change*	1.12	16.02

Table 3: DSC data for both control and the Biofield Energy Treated samples of  $\text{CrO}_3$  powder.

$\Delta H$ : Latent heat of fusion, \*denotes the percentage change of the Biofield Energy Treated  $\text{CrO}_3$  powder with respect to the control sample.

## Conclusion

The experimental results concluded that the Trivedi Effect®-Consciousness Energy Healing Treatment have a substantial impact on the particle size, surface area, crystallite, and thermal properties of  $\text{CrO}_3$ . The particle size values of the Consciousness Energy Healing Treated  $\text{CrO}_3$  were increased by 71.13%, 2.09%, and 0.03% at  $d_{10}$ ,  $d_{50}$ , and  $D(4, 3)$ , respectively and decreased by 10.86% at  $d_{90}$  compared to the control sample. Hence, the specific surface area of the treated  $\text{CrO}_3$  was significantly decreased by 63.76% compared with the control sample. The PXRD diffractograms of the control and Consciousness Energy Healing Treated  $\text{CrO}_3$  showed sharp and intense peaks indicated that both the samples were crystalline. The peak intensities of the treated  $\text{CrO}_3$  were significantly altered ranging from -27.64% to 30.72% compared with the control sample. Similarly, the crystallite sizes of the Consciousness Energy Healing Treated sample were significantly altered ranging from -46.14% to 136.44% compared to the control sample. Overall, the average crystallite size of the Consciousness Energy Healing Treated  $\text{CrO}_3$  was significantly increased by 17.65% compared with the control sample. The  $\Delta H_{\text{fusion}}$  the Consciousness Energy Healing Treated  $\text{CrO}_3$  was significantly increased by 16.02% compared with the control sample. The experimental results indicated that the Trivedi Effect®-Consciousness Energy Healing Treatment might have included a new polymorphic form of  $\text{CrO}_3$  which may be better powder flowability and lower solubility. Thus, it may lower the absorption and toxicity

of  $\text{CrO}_3$  on inhalation, ingestion, contact to skin and eye, chronic exposure, and aggravation of pre-existing conditions. As well the Dahryn's Consciousness Energy Healing Treated  $\text{CrO}_3$  would be very useful for the industry manufacturing the synthetic rubies, aerospace parts, stripping agent of anodic coatings, etc.

## Acknowledgement

The authors are grateful to Central Leather Research Institute, SIPRA Lab. Ltd., Trivedi Science, Trivedi Global, Inc., Trivedi Testimonials, and Trivedi Master Wellness for their assistance and support during this work.

## References

- <http://www.chemicaland21.com/industrialchem/inorganic/CHROMIUM%20TRIOXIDE.htm><http://www.chemicaland21.com/industrialchem/inorganic/CHROMIUM%20TRIOXIDE.htm> Retrieved 2015-06-2018.
- [https://en.wikipedia.org/wiki/Chromium\\_trioxide](https://en.wikipedia.org/wiki/Chromium_trioxide). Retrieved 15-06-2018.
- Anger G, Halstenberg J, Hochgeschwender K, Scherhag C, Korallus U, et al. (2000) Chromium Compounds. Ullmann's Encyclopedia of Industrial Chemistry.
- MacInnis, Daniel (1973) Synthetic Gem and Allied Crystal Manufacture. Park Ridge, NJ: Noyes Data Corporation.
- Lucia O, Mihaela P, Stela C, Camelia T, Corina G, et al. (2010) Deuterium depleted water behavior in chromium (VI) intoxicated female rats'. Banat's Journal of Biotechnology 1(1): 72-75.
- Trivedi MK, Branton A, Trivedi D, Nayak G, Wellborn BD, et al. (2017) Characterization of physical, structural, thermal, and behavioral properties of the consciousness healing treated zinc chloride. World Journal of Applied Chemistry 2(2): 57-66.
- Trivedi MK, Branton A, Trivedi D, Nayak G, Lee AC, et al. (2017) investigation of physicochemical, spectral, and thermal properties of sodium selenate treated with the Energy of Consciousness (the Trivedi Effect®). American Journal of Life Sciences 5(1): 27-37.
- Trivedi MK, Branton A, Trivedi D, Nayak G, Wellborn BD, et al. (2017) Characterization of physicochemical, thermal, structural, and behavioral properties of magnesium gluconate after treatment with the

- Energy of Consciousness. International Journal of Pharmacy and Chemistry 3(1): 1-12.
9. Trivedi MK, Branton A, Trivedi D, Nayak G, Gangwar M, et al. (2015) Agronomic characteristics, growth analysis, and yield response of biofield treated mustard, cowpea, horse gram, and groundnuts. International Journal of Genetics and Genomics 3(6): 74-80.
  10. Trivedi MK, Mohan TRR (2016) Biofield energy signals, energy transmission and neutrinos. American Journal of Modern Physics 5(6): 172-176.
  11. Rubik B, Muehsam D, Hammerschlag R, Jain S (2015) Biofield science and healing: history, terminology, and concepts. Glob Adv Health Med 4(Suppl): 8-14.
  12. Barnes PM, Bloom B, Nahin RL (2008) Complementary and alternative medicine use among adults and children: United States, 2007. Natl Health Stat Report 12: 1-23.
  13. Koithan M (2009) Introducing complementary and alternative therapies. J Nurse Pract 5(1): 18-20.
  14. Trivedi MK, Tallapragada RM, Branton A, Trivedi D, Nayak G, et al. (2015) Evaluation of physical and structural properties of biofield energy treated barium calcium tungsten oxide. Advances in Materials 4(6): 95-100.
  15. Trivedi MK, Tallapragada RM, Branton A, Trivedi D, Nayak G, et al. (2015) Evaluation of atomic, physical, and thermal properties of bismuth oxide powder: An impact of biofield energy treatment. American Journal of Nano Research and Applications 3: 94-98.
  16. Trivedi MK, Branton A, Trivedi D, Nayak G, Sethi KK, et al. (2016) Isotopic abundance ratio analysis of biofield energy treated indole using gas chromatography-mass spectrometry. Science Journal of Chemistry 4(4): 41-48.
  17. Trivedi MK, Branton A, Trivedi D, Nayak G, Panda P, et al. (2016) Evaluation of the isotopic abundance ratio in biofield energy treated resorcinol using gas chromatography-mass spectrometry technique. Pharm Anal Acta 7: 481.
  18. Trivedi MK, Branton A, Trivedi D, Nayak G, Saikia G, et al. (2015) Physical and structural characterization of biofield treated imidazole derivatives. Nat Prod Chem Res 3(5): 187.
  19. Branton A, Jana S (2017) Effect of The biofield energy healing treatment on the pharmacokinetics of 25-hydroxyvitamin D<sub>3</sub> [25(OH)D<sub>3</sub>] in rats after a single oral dose of vitamin D<sub>3</sub>. American Journal of Pharmacology and Phytotherapy 2(1): 11-18.
  20. Trivedi MK, Branton A, Trivedi D, Nayak G, Mondal SC, et al. (2015) Evaluation of plant growth, yield and yield attributes of biofield energy treated mustard (*Brassica juncea*) and chick pea (*Cicer arietinum*) seeds. Agriculture, Forestry and Fisheries 4(6): 291-295.
  21. Trivedi MK, Branton A, Trivedi D, Nayak G, Mondal SC, et al. (2015) Evaluation of plant growth regulator, immunity and DNA fingerprinting of biofield energy treated mustard seeds (*Brassica juncea*). Agriculture, Forestry and Fisheries. 4(6): 269-274.
  22. Trivedi MK, Branton A, Trivedi D, Nayak G, Bairwa K, et al. (2015) Physical, thermal, and spectroscopic characterization of biofield energy treated murashige and skoog plant cell culture media. Cell Biology 3(4): 50-57.
  23. Trivedi MK, Branton A, Trivedi D, Nayak G, Mondal SC, et al. (2015) Antimicrobial sensitivity, biochemical characteristics and biotyping of *Staphylococcus saprophyticus*: An impact of biofield energy treatment. J Women's Health Care 4: 271.
  24. Trivedi MK, Branton A, Trivedi D, Nayak G, Shettigar H, et al. (2015) AntibioGram of multidrug-resistant isolates of *Pseudomonas aeruginosa* after biofield treatment. J Infect Dis Ther 3: 244.
  25. Trivedi MK, Patil S, Shettigar H, Mondal SC, Jana S (2015) The potential impact of biofield treatment on human brain tumor cells: A time-lapse video microscopy. J Integr Oncol 4: 141.
  26. Trivedi MK, Sethi KK, Panda P, Jana S (2017) A comprehensive physicochemical, thermal, and spectroscopic characterization of zinc (II) chloride using X-ray diffraction, particle size distribution, differential scanning calorimetry, thermogravimetric analysis/differential thermogravimetric analysis, ultraviolet-visible, and Fourier transform-infrared spectroscopy. Int J Pharm Investig 7(1): 33-40.
  27. Trivedi MK, Sethi KK, Panda P, Jana S (2017) Physicochemical, thermal and spectroscopic characterization of sodium selenate using XRD, PSD, DSC, TGA/DTG, UV-vis, and FT-IR. Marmara Pharmaceutical Journal 21(2): 311-318.

28. Michael G Rosamann (1997) Desktop X-ray Diffractometer "MiniFlex+". The Rigaku Journal 14: 29-36.
29. Zhang T, Paluch K, Scalabrino G, Frankish N, Healy AM, et al. (2015) Molecular structure studies of (1S,2S)-2-benzyl-2,3-dihydro-2-(1Hinden-2-yl)-1H-inden-1-ol. J Mol Struct 1083: 286-299.
30. Langford JI, Wilson AJC (1978) Scherrer after sixty years: A survey and some new results in the determination of crystallite size. J Appl Cryst 11: 102-113.
31. Rodino S, Butu M, Gaidau C, Calin M, Butu A (2017) Ontological model for the evaluation of the impact of nanoparticles on the human cell morphology. Banat's Journal of Biotechnology VIII: 18-23.
32. Buckton G, Beezer AE (1992) The relationship between particle size and solubility. Int J Pharmaceutics 8 2(3): R7-R10.
33. Inoue M, Hirasawa I (2013) The relationship between crystal morphology and XRD peak intensity on CaSO<sub>4</sub>.2H<sub>2</sub>O. J Crystal Growth 380: 169-175.
34. Raza K, Kumar P, Ratan S, Malik R, Arora S (2014) Polymorphism: The phenomenon affecting the performance of drugs. SOJ Pharm Pharm Sci 1(2): 10.
35. Brittain HG (2009) Polymorphism in pharmaceutical solids. Drugs and Pharmaceutical Sciences, (2<sup>nd</sup> edn), volume 192, Informa Healthcare USA, Inc., New York.
36. Censi R, Di Martino P (2015) Polymorph Impact on the Bioavailability and stability of poorly soluble drugs. Molecules 20(10): 18759-18776.
37. Blagden N, de Matas M, Gavan PT, York P (2007) Crystal engineering of active pharmaceutical ingredients to improve solubility and dissolution rates. Adv Drug Deliv Rev 59(7): 617-630.
38. Zhao Z, Xie M, Li Y, Chen A, Li G, et al. (2015) Formation of curcumin nanoparticles *via* solution-enhanced dispersion by supercritical CO<sub>2</sub>. Int J Nanomedicine 10: 3171-3181.